New Phytologist

Research

Arabidopsis thaliana B-GATA factors repress starch synthesis and gravitropic growth responses

Jan Sala[1], Niccolò Mosesso[2], Erika Isono[2] and Claus Schwechheimer[1]

[1]Plant Systems Biology, Technische Universität München, Emil-Ramann-Strasse 8, 85354 Freising, Germany; [2]Plant Physiology and Biochemistry, Department of Biology, University of Konstanz, 78457 Constance, Germany

Author for correspondence:
Claus Schwechheimer
Email: claus.schwechheimer@tum.de

Received: *6 February 2023*
Accepted: *26 April 2023*

New Phytologist (2023) **239:** 979–991
doi: 10.1111/nph.18992

Key words: amyloplast, GATA factor, gravitropism response, starch, starch granule.

Summary

- Plants perceive the direction of gravity during skotomorphogenic growth, and of gravity and light during photomorphogenic growth. Gravity perception occurs through the sedimentation of starch granules in shoot endodermal and root columella cells. In this study, we demonstrate that the *Arabidopsis thaliana* GATA factors *GNC* (*GATA*, *NITRATE-INDUCIBLE*, *CARBON METABOLISM-INVOLVED*) and *GNL/CGA1* (*GNC-LIKE/CYTOKININ-RESPONSIVE GATA1*) repress starch granule growth and amyloplast differentiation in endodermal cells.
- In our comprehensive study, we analysed gravitropic responses in the shoot, root and hypocotyl. We performed an RNA-seq analysis, used advanced microscopy techniques to examine starch granule size, number and morphology and quantified transitory starch degradation patterns. Using transmission electron microscopy, we examined amyloplast development.
- Our results indicate that the altered gravitropic responses in hypocotyls, shoots and roots of *gnc gnl* mutants and GNL overexpressors are due to the differential accumulation of starch granules observed in the *GATA* genotypes. At the whole-plant level, *GNC* and *GNL* play a more complex role in starch synthesis, degradation and starch granule initiation.
- Our findings suggest that the light-regulated *GNC* and *GNL* help balance phototropic and gravitropic growth responses after the transition from skotomorphogenesis to photomorphogenesis by repressing the growth of starch granules.

Introduction

Plants convert carbon dioxide and water into sugars through photosynthesis. During skotomorphogenic growth, seedling roots grow towards the gravity vector, referred to as positive gravitropism, while their hypocotyls elongate away from gravity to reach the light, referred to as negative gravitropism (Kiss, 2000; Sato *et al.*, 2015). According to the starch–statolith hypothesis, starch-filled amyloplasts, or statoliths, sediment in the hypocotyl endodermis or in the root columella during the perception of gravity and generate a signal that causes asymmetric growth (Kiss *et al.*, 1989; Christie & Murphy, 2013). The strength of these gravitropic responses is, amongst others, dependent on the size of the starch granules, which increases in response to sugar availability (Kiss *et al.*, 1998). In the light, plants also use phototropism, mediated by phototropin blue light receptors, to orient their growth towards the light for optimal photosynthesis (Briggs & Christie, 2002; Christie & Murphy, 2013). When the respective inputs do not act in the same direction, plants have to find a balance between phototropic and gravitropic growth (Hangarter, 1997).

Starch consists of amylose and amylopectin (Zeeman *et al.*, 2002). Amylose is composed of linear chains of α-1,4-linked D-glucose residues, whereas amylopectin is branched through additional α-1,6-linked D-glucoses (Seung, 2020). Amylose synthesis is achieved by the activity of GRANULE BOUND STARCH SYNTHASE1 (GBSS1), whereas amylopectin synthesis requires soluble starch synthases (SS) and two types of branching enzymes (BE; Delvalle *et al.*, 2005; Zhang *et al.*, 2008; Lu *et al.*, 2015; Seung *et al.*, 2020; Gamez-Arjona & Merida, 2021). Granule initiation involves the coordination of a specialised set of proteins, including SS4, which determines granule shape and number through the interaction with PROTEIN TARGETING TO STARCH (PTST; Roldan *et al.*, 2007; Seung *et al.*, 2018).

Starch degradation encompasses, first, the activity of glucan water dikinases (GWDs) that phosphorylate the starch granule surface, subsequently allowing α-amylases (AMY) and β-amylases (BAM) to hydrolyse the nonreducing ends of the starch molecules (Yu *et al.*, 2001; Flutsch *et al.*, 2020; Feike *et al.*, 2022). *sex1* (*starch excess1*) mutants accumulate high amounts of starch due to a defect in *GWD1* function (Yu *et al.*, 2001).

GATA factors are evolutionarily conserved transcription factors (Schwechheimer *et al.*, 2022). GNC (GATA, NITRATE-INDUCIBLE, CARBON METABOLISM-INVOLVED) and GNL/CGA1 (GNC-LIKE/CYTOKININ-RESPONSIVE GATA1)

are two prominent members among the six so-called LLM-domain B-GATAs from *Arabidopsis thaliana* (Bi *et al.*, 2005; Naito *et al.*, 2007). *GNC* and *GNL* are light-regulated and act redundantly in the regulation of chlorophyll biosynthesis and chloroplast division, as well as stomata formation (Bi *et al.*, 2005; Naito *et al.*, 2007; Chiang *et al.*, 2012; Klermund *et al.*, 2016; Ranftl *et al.*, 2016; Bastakis *et al.*, 2018). While the gradual loss of the six Arabidopsis LLM-domain B-GATAs results in a gradual increase in the strengths of the respective phenotypes, the antagonistic phenotype is generally observed when the GATAs are overexpressed, arguing for a strong dosage-dependency of GATA-controlled biological processes (Behringer *et al.*, 2014; Klermund *et al.*, 2016). One such gene dosage-dependent phenotype is the change in the angle of lateral shoots emerging from the primary inflorescence in *GATA* gene mutants and overexpressors (Richter *et al.*, 2010; Ranftl *et al.*, 2016). The molecular basis of this phenotype remains to be understood.

In this study, we reveal a prominent role of *GNC* and *GNL* as repressors of starch granule growth and amyloplast differentiation, in cell types required for the perception of gravity. Based on the light-regulation of *GNC* and *GNL* transcription, we postulate that they help balancing between phototropic and gravitropic growth responses after the transition from skotomorphogenic to photomorphogenic growth.

Materials and Methods

Biological material

All experiments were performed in *Arabidopsis thaliana* L. ecotype Columbia (Col-0). The *gnc* (SALK_001778) and *gnl* (SALK_003995) single and double mutants, as well as the GNL overexpression line GNLox were previously described (Richter *et al.*, 2010). *sex1-8* (SALK_077211) and *ss4-1* (SALK_096130) were obtained from the Nottingham Arabidopsis Stock Centre (NASC; Roldan *et al.*, 2007; Mahlow *et al.*, 2014). Homozygous mutant combinations were isolated from segregating populations by PCR-based genotyping with oligonucleotides (Supporting Information Table S1).

Seedlings were cultivated on sterile half-strength Murashige & Skoog (½MS) medium (Duchefa, Harlem, the Netherlands), when specified supplemented with sucrose. For tropism experiments, seedlings were, unless specified otherwise, grown in the dark in growth chambers at 21°C. When grown in the light, all plants were grown in growth chambers at 21°C under white-fluorescent light (120 $\mu mol\ m^{-2}\ s^{-1}$) with a 16 h : 8 h, light : dark photoperiod.

Tropism assays

For seedling gravitropism assays, seedlings were grown for 2 d in the dark on vertically oriented ½MS plates. Since the genotypes examined here affected hypocotyl growth in the dark due to defects in negative gravitropism, seedling hypocotyls were straightened, away from the gravity vector, in safe green light, before the plates were turned by 90° and grown for an additional 24 h. Subsequently, photographs were taken with a Sony A6100 digital camera (Sony, Berlin, Germany) and the bending of hypocotyls and root tips was measured from the digital images using the Fiji ImageJ software (Schindelin *et al.*, 2012). Because cotyledon position influences the degree of negative hypocotyl gravitropism, only seedlings with their cotyledons pointing in the bending direction were included in the quantification (Khurana *et al.*, 1989).

For stem gravitropism, plants were grown in a growth chamber on soil until their primary inflorescences reached 10 cm. Then, plants were placed horizontally for an hour in a dark-chamber to determine negative shoot gravitropism and to prevent interference from phototropic responses. Inflorescence bending was determined from digital photographs as described above.

To determine the interaction between hypocotyl-negative gravitropism and phototropism, seedlings were grown for 2 d in the dark on vertically oriented plates with ½MS, and straightened as described above. Plates were then turned by 90° and grown for 6 h with unilateral blue light illumination (1 $\mu mol\ m^{-2}\ s^{-1}$) from above or below, as specified. Seedling bending was determined from digital photographs as described above.

RNA-seq

For RNA-seq, wild-type (Col-0), *gnc gnl* and GNLox seedlings were grown in the dark on ½MS medium for 3 d. Liquid nitrogen-frozen seedlings were disrupted in a Tissue Lyser2 (Qiagen) and total RNA was extracted using a NucleoSpin RNA kit (Macherey-Nagel, Düren, Germany). RNA quantity and quality were determined with a 2100 Bioanalyzer (Agilent, Santa Cara, CA, USA). Libraries were generated with the Illumina stranded mRNA Kit (Illumina, San Diego, CA, USA) and single-ended sequencing was performed on a NovaSeq 6000 (Illumina). Reads were mapped to the region of the TAIR10 release of the *Arabidopsis thaliana* Col-0 genome (www.arabidopsis.org) using the default settings of the CLC Genomics Workbench (Qiagen). Differentially expressed genes were filtered by a false discovery rate (FDR) < 0.05. The RNA-seq data are available at Gene Expression Omnibus (https://www.ncbi.nlm.nih.gov/geo/) under accession number GSE205524.

Gene ontology analysis was performed using the PANTHER algorithm at TAIR and the enriched set of differentially expressed genes was retrieved according to their biological function (Lamesch *et al.*, 2012). The list of genes of genes was then uploaded to the STRING database in order to annotate the corresponding protein–protein interactions (Szklarczyk *et al.*, 2017). Networks were built using the Cytoscape software (Shannon *et al.*, 2003).

Confocal laser scanning microscopy

Confocal laser scanning microscopy was performed with an Olympus FV1000 using an excitation wavelength of 488 nm and emission at 520–720 nm, after cell wall- and starch granule-staining with mPS-PI (modified pseudo-Schiff reagent-

propidium iodide; Truernit *et al.*, 2008). Starch granule size was measured from the digital images using the FIJI IMAGEJ software (Schindelin *et al.*, 2012), considering the starch granule area (μm^2), as a proxy for starch granule size of individual starch granules. High-magnification images of mPS-PI stained starch granules allowed to distinguish between several starch granules in one amyloplast.

Light microscopy

For the imagining of starch distribution, 3-d-old dark-grown seedlings were stained for 1 min with Lugol's solution, and destained for 5 min with distilled water. Stained seedlings were mounted and imaged with an Olympus BX61 light microscope (Olympus, Shinjuku, Tokio, Japan). For the imaging of starch granules by light microscopy, starch granule preparations were dispersed in distilled water, stained with Lugol's solution and glycerol (1 : 1, v/v) and imaged as described above.

Starch quantification

Starch was quantified with the Megazyme Total Starch HK Assay Kit (Megazyme, Bray, Ireland) from 200 mg liquid nitrogen-frozen seedlings harvested at specified time points. Plant material was disrupted until homogeneous with a Tissue Lyser2 (Qiagen). The tissue was then incubated in 80% ethanol for 5 min, and insoluble material pelleted by centrifugation at 10 000 ***g*** for 5 min. The supernatant was discarded and the ethanol extraction was repeated once. The starch-containing pellet was transferred to a 15-ml glass tube and starch quantification was performed according to the manufacturer's instructions (Megazyme).

Purification of starch granules

Starch granules were purified from liquid nitrogen-frozen entire 3-d-old dark-grown seedlings. Seedlings were homogenized with a tissue blender in 2 ml of ice-cold extraction buffer (50 mM Tris–HCl, pH 8.0; 0.2 mM EDTA, 0.5% Triton X-100). The homogenate was filtered through Miracloth (Merck, Darmstadt, Germany) and pelleted by centrifugation at 2500 ***g*** for 15 min. The pellet was resuspended in 1 ml of extraction buffer, containing 0.5% SDS (sodium dodecyl-sulfate). Subsequently, the pellet was washed five times with distilled water and repelleted by centrifugation at 2500 ***g*** for 10 min to remove excess SDS.

Scanning electron microscopy

For scanning electron microscopy, starch granules were sputter-coated for 90 s with a gold alloy and imaged at 5.0 kV in a Jeol JSM-7200F field emission scanning electron microscope.

Transmission electron microcopy

Hypocotyls from 5-d-old dark-grown Arabidopsis seedlings were high-pressure frozen in a Leica EM ICE high-pressure freezer (Leica, Wetzlar, Germany). Frozen samples were freeze-substituted in a Leica EM AFS2 (Leica) in 2.5% OsO_4 in acetone for 41 h at −90°C. Subsequently, the temperature was gradually increased to 0°C. Hypocotyls were then infiltrated with Epoxy Embedding Medium (EPON; Fluka Chemie, Buchs, Switzerland) for ultrastructural analyses. A total of 70 nm ultra-thin sections were mounted on copper grids (Plano GmbH, Wetzlar, Germany) coated with Pioloform (Wacker-Chemie, Munich, Germany) and stained with saturated Uranyl Acetate (Merck) at 4°C, followed by 0.4% lead citrate in 0.2% NaOH. Alternatively, samples were stained with UranyLess (Science Services, Munich, Germany) and 0.4% lead citrate in 0.2% NaOH. The sections were imaged in a Jeol 2100 Plus electron microscope (Jeol, Freising, Germany) operated at 120 kV.

Results

GNC and *GNL* repress negative shoot gravitropism

We have previously reported that the lateral shoots of *Arabidopsis thaliana gnc gnl* mutants emerge with a steeper angle (< 60°) from the primary inflorescence than in the wild-type (*c.* 65°), whereas the lateral shoot angles in *GATA* overexpression lines, such as GNLox, are strongly increased (*c.* 85°; Richter *et al.*, 2010; Behringer *et al.*, 2014; Ranftl *et al.*, 2016). To examine whether these defects were related to defects in shoot negative gravitropic response, we measured the shoot gravitropism response of 25-d-old wild-type, *gnc gnl* and GNLox inflorescences 1 h after turning them by 90° (Fig. 1a). To avoid interference from phototropic responses, the experiment was performed in the dark. While the wild-type plant had reoriented its inflorescence after 1 h by *c.* 60°, the *gnc gnl* double mutant had already fully reoriented to 90°, whereas the GNLox inflorescence had reoriented only by *c.* 30° (Fig. 1a,b). When we analysed negative gravitropism in hypocotyls of 2-d-old *gnc gnl* and GNLox seedlings grown in the dark on ½MS medium, the hypocotyl bending angle was increased in *gnc gnl* and decreased in GNLox, when compared to the wild-type (Fig. 1c–e). Addition of 1% sucrose to the medium enhanced the gravitropism response in all three genotypes, but the respective differential gravitropic responses were maintained (Fig. 1d,e). *GNC* and *GNL* thus repress negative gravitropism. When we analysed the positive gravitropism of seedling roots, root bending in *gnc gnl* mutants was subtly increased compared with the wild-type, but this difference became more pronounced and statistically significant on sucrose-containing medium (Fig. 1f). *GNC* and *GNL* thus also repress positive root gravitropism.

Starch metabolism genes are upregulated in dark-grown *gnc gnl* mutant seedlings

Graviperception induces negative gravitropism in the endodermis of hypocotyls and shoots and positive gravitropism in root columella cells, thus responses that were affected in the *GATA* genotypes (Christie & Murphy, 2013). Since gravity perception is promoted by the sedimentation of starch-filled amyloplasts, the differential regulation of starch metabolism genes may explain the differential gravitropism responses of the *GATA* genotypes

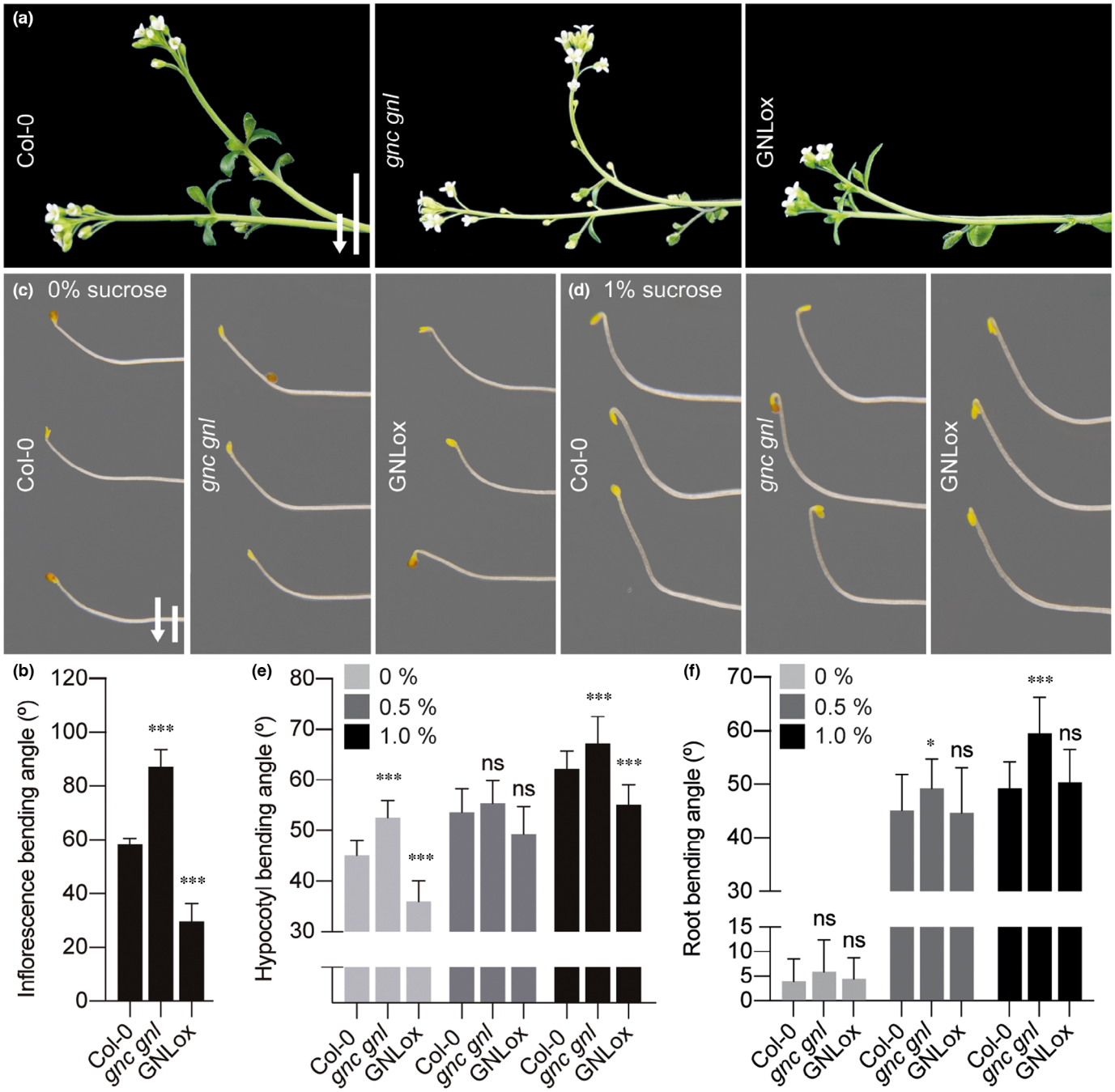

Fig. 1 *GNC* and *GNL* repress negative gravitropism in the shoot and the hypocotyl and positive gravitropism in the root. (a) Overlay of two representative photographs of 25-d-old *Arabidopsis thaliana* wild-type (Col-0), *gnc gnl* and GNLox inflorescences before (horizontally oriented shoots) and 1 h after turning the plants by 90° (upward bent shoots). The arrow indicates the direction of the gravity vector. Bar, 1 cm. (b) Average and standard deviation of inflorescence bending angles as detected in the experiment shown in (a) and measured from 10 wild-type, *gnc gnl* or GNLox plants. (c, d) Representative photographs of *Arabidopsis thaliana* wild-type (Col-0), *gnc gnl* and GNLox hypocotyls from 2-d-old seedlings grown on sucrose-free Murashige & Skoog (½MS) medium (c) and 1% sucrose-supplemented ½MS medium (d), as specified, 24 h after reorienting the seedlings by 90°. The arrow indicates the direction of the gravity vector. Bar, 1 mm. (e) Average and standard deviation of the hypocotyl bending angle as detected in the experiment shown in (c) from 40 wild-type, *gnc gnl* or GNLox seedlings. (f) Average and standard deviation of the root bending angle from 50 wild-type, *gnc gnl* or GNLox seedlings 24 h after turning the seedlings by 90°. Student's *t*-test: *, $P \leq 0.05$; ***, $P \leq 0.001$; ns, not significant.

(Kiss *et al.*, 1989; Christie & Murphy, 2013). To examine whether starch-related genes were differentially regulated in *gnc* gnl and GNLox, we performed an RNA-seq analysis with entire wild-type, *gnc gnl* and GNLox seedlings grown in the dark for 3 d on ½MS medium. Applying a false discovery rate (FDR) < 0.05, we identified 1876 up- and 1312 downregulated genes in *gnc gnl*, as well as 2046 up- and 2204 downregulated genes in GNLox when compared to the wild-type (Table S2).

A gene ontology (GO) analysis identified 'Photosynthesis' (9.65-fold enrichment), 'Starch metabolism' (5.43) and 'Stomata development' (4.44) as the three most important GO categories from genes upregulated in *gnc gnl* (Fig. 2a,b; Table S3; Ashburner *et al.*, 2000; Gene Ontology, 2021). The majority of genes belonging to the term category 'Photosynthesis' accounted for *LIGHT HARVESTING COMPLEX* (*LHC*), whereas genes associated with the term category 'Porphyrin metabolism', such as *NON-YELLOW COLORING 1* (*NYC1*), were downregulated. While our analysis cannot state whether *LHC* genes are directly regulated by GNC and GNL, it is plausible that differences in *LHC* transcript levels are a result of feedback regulatory mechanisms involving the GATA factors, since these had previously been implicated in greening regulation (Bastakis *et al.*, 2018). Furthermore, the regulation of genes involved in porphyrin metabolism and stomata development is consistent with the well-established roles of *GNC* and *GNL* in both, chlorophyll metabolism and stomata development (Chiang *et al.*, 2012; Klermund *et al.*, 2016; Ranftl *et al.*, 2016; Bastakis *et al.*, 2018; Zubo *et al.*, 2018).

Among the genes belonging to the term category 'Starch metabolism', we detected an increased expression of *PHOSPHOGLUCOMUTASE* (*PGM*), of three genes encoding for the large (*APL*) or small (*APS*) subunits of ADP-glucose pyrophosphorylase, of *GBSS1*, as well as *SEX4* (Fig. 2c; Table S3). More important, *SS1*, *BE1* and *ISA2* were antagonistically regulated between the double mutant and GNLox. Upregulation of these genes in *gnc gnl* may lead to increased starch synthesis and differential starch accumulation may be causal for the tropism phenotypes of *gnc gnl* and, conversely, in GNLox (Figs 1c–f, 2c).

Starch granule size and number are altered in *gnc gnl* and GNLox

We next examined starch granule size and number in the hypocotyl endodermis and in root columella cells of dark-grown wild-type, *gnc gnl* and GNLox seedlings grown on sucrose-free or sucrose-containing medium (Fig. 3; Truernit *et al.*, 2008). We detected a subtle increase in *gnc* and *gnl* single mutants, which became more apparent in *gnc gnl*, and a particularly strong decrease in GNLox starch granule size in hypocotyl endodermal as well as in root columella cells (Figs 3a–f, S1). On sucrose-containing medium (1% sucrose), starch granule size increased in all genotypes but the respective differences between the three genotypes were maintained, but quantitatively strongly enhanced in GNLox. Therefore, we concluded that the *GATAs* repress starch granule growth in gravity-sensing cells (Fig. 3a–f).

At the same time, we noticed that the number of starch granules was strongly increased in GNLox endodermis cells and slightly, but insignificantly, decreased in *gnc*, *gnl* and *gnc gnl*, suggesting that GATAs may promote starch granule initiation in the endodermis (Figs 3g, S1). On the contrary, granule number was strongly decreased in root columella cells of GNLox grown on sucrose-free medium, whereas *gnc gnl* mutants accumulated a significantly increased number of starch granules on this medium (Fig. 3h). On 1% sucrose, all genotypes produced more starch granules than on sucrose-free medium and the differences between the genotypes disappeared (Fig. 3h). We thus noted that the effects of GATAs on starch granule size, but not those on starch granule number, are consistent between the two tissue types examined here.

GNC and *GNL* may repress starch granule growth in a *SEX1*- and *SS4*-depdendent manner

Starch degradation is initiated trough amylopectin phosphorylation by *GWD*s, thus impaired starch degradation in the *GWD1* mutant *sex1* leads to starch accumulation (Yu *et al.*, 2001). Furthermore, uneven metabolism at the granule surface results in irregular edges of starch granules (Edner *et al.*, 2007; Liu *et al.*, 2021b). On the contrary, *SS4* promotes starch granule initiation and determines starch granule number, while also having an influence on granule shape (Crumpton-Taylor *et al.*, 2013; Merida & Fettke, 2021). In contrast to the multiple flatter granules found in wild-type plants, *ss4* mutants produce only one round granule per amyloplast. Taking into consideration the available literature, we introduced the *sex1* and *ss4* mutants into the *GATA* mutant and overexpression lines to better understand the role of *GNC* and *GNL* in starch granule growth in hypocotyl endodermal and root columella cells (Yu *et al.*, 2001; Edner *et al.*, 2007; Crumpton-Taylor *et al.*, 2013; Merida & Fettke, 2021; Liu *et al.*, 2021b).

In the root cap, the size of starch granules in the *sex1* background did not increase compared to the wild-type, when grown on sucrose-free ½MS medium (Fig. S2c,g). Whereas we could not observe significant differences in starch granule size between *sex1* and *sex1 gnc gnl*, we detected a decrease in *sex1* GNLox, compared with both *sex1* and the wild-type (Fig. S2c,g). On 1% sucrose-supplemented medium, starch granule size increased in *sex1*, *sex1 gnc gnl* and *sex1* GNLox (Fig. S2c,d,g). We noted a subtle, but not significant increase in *sex1 gnc gnl* compared to *sex1*, and a more pronounced decrease in *sex1 GNLox* compared with *sex1* (Fig. S2d,g). In addition, the roots of *sex1* seedlings grown in the dark exhibited a higher accumulation of starch granules compared with the wild-type (Fig. S2a–d,h). After mPS-PI staining and subsequent quantification, no significant differences were observed between *sex1* and *sex1 gnc gnl*, while the number of starch granules in *sex1* GNLox increased (Fig. S2c,h). Interestingly, starch granules were mostly found in columella cells in *sex1*, whereas starch granules also accumulated in other cell files in *sex1* GNLox, such as lateral, cortex and epidermal cells (Figs S2c,d, S3). On 1% sucrose, *sex1*, *sex1 gnc gnl* and *sex1* GNLox accumulated starch in most cell files (Fig. S2d,h). The absence of starch granules in noncolumella wild-type and *sex1* cells may be due to increased starch turnover in these cells.

In the root cap of *ss4* seedlings, starch granules exhibited the previously described round morphology and were notably larger than those observed in the wild-type (Fig. S2a,b,e–g; Merida & Fettke, 2021). The size of starch granules was strongly increased in *ss4 gnc gnl*, and particularly in *ss4* GNLox (Fig. S2e–g). On sucrose-supplemented ½MS medium, starch granules in *ss4 gnc gnl* and *ss4* GNLox were 10 times larger than those of the wild-

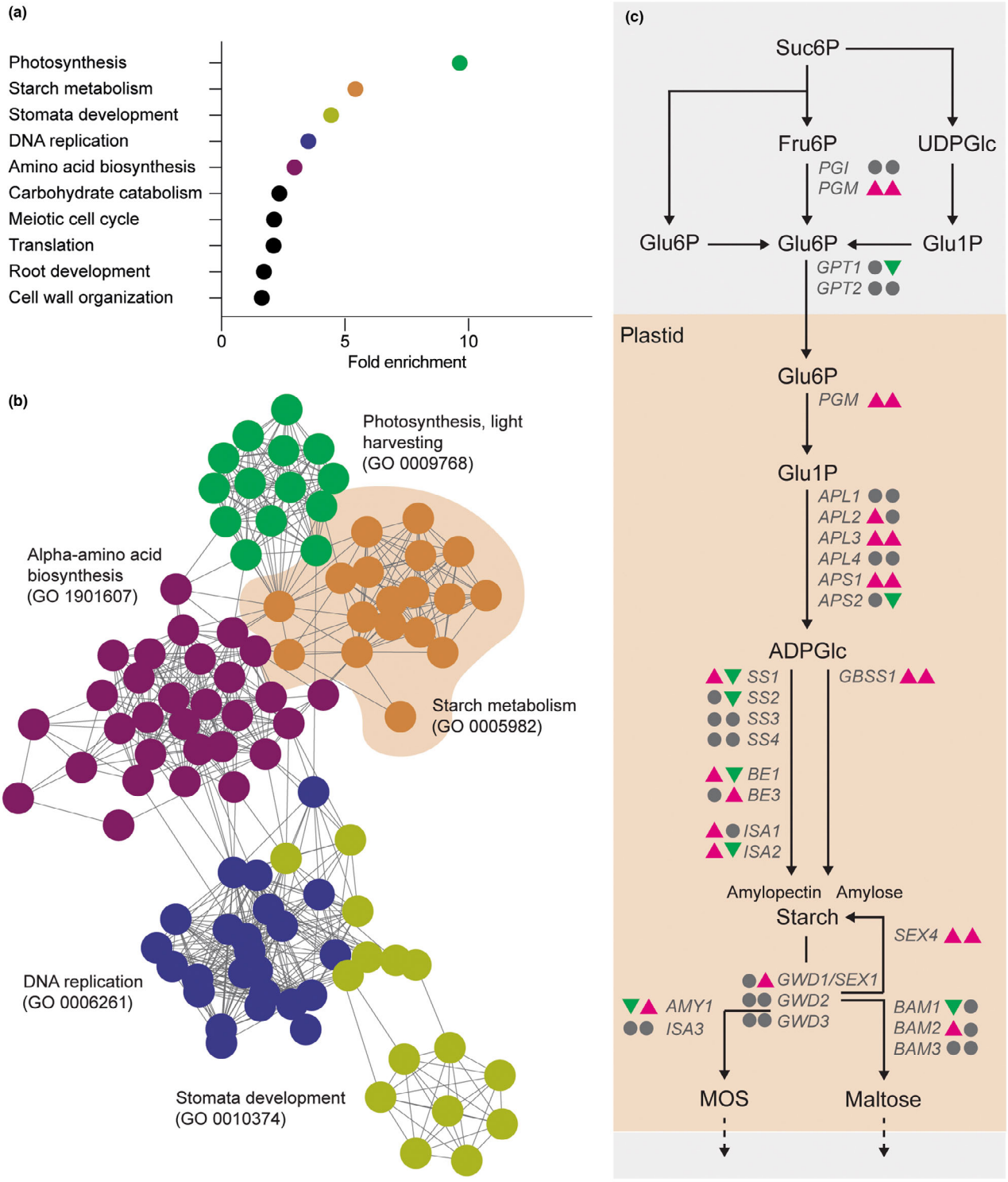

Fig. 2 Starch metabolism genes are differentially regulated in dark-grown *gnc gnl* seedlings. (a) Graph displaying the gene ontology (GO) terms enrichment of the 10 most strongly regulated GO term categories among the genes upregulated in *gnc gnl*. (b) STRING network analysis of the genes belonging to the five most prominent GO term categories as shown in (a). (c) Graphical display of the starch anabolism and catabolism pathway. Arrowheads symbolize genes upregulated (magenta) or downregulated (green) in *gnc gnl* (left) and GNLox (right) using false discovery rate (FDR) < 0.5 as c Information Table S2). ADPGlc, ADP-glucose; AMY, alpha-amylase; APL, ADP-glucose pyrophosphorylase large subunit; APS, ADP-glucose pyrophosphorylase small subunit; BAM, beta-amylase; BE, branching enzyme; Fru6P, fructose-6-phosphate; GBSS, granule-bound starch synthase; Glu1P, glucose-1-phosphate; Glu6P, glucose-6-phosphate; GPT1, glucose 6-phosphate translocator; GWD, glucan water dikinase; ISA, isoamylase; MOS, maltooligosaccharides; PGI, phosphoglucose isomerase; PGM, phosphoglucomutase; SEX1, starch excess1; SEX4, starch excess4/laforin-like1 phosphoglucan phosphatase; SS, starch synthase; Suc6P, sucrose-6-phosphate; UDPGlc, UDP-glucose.

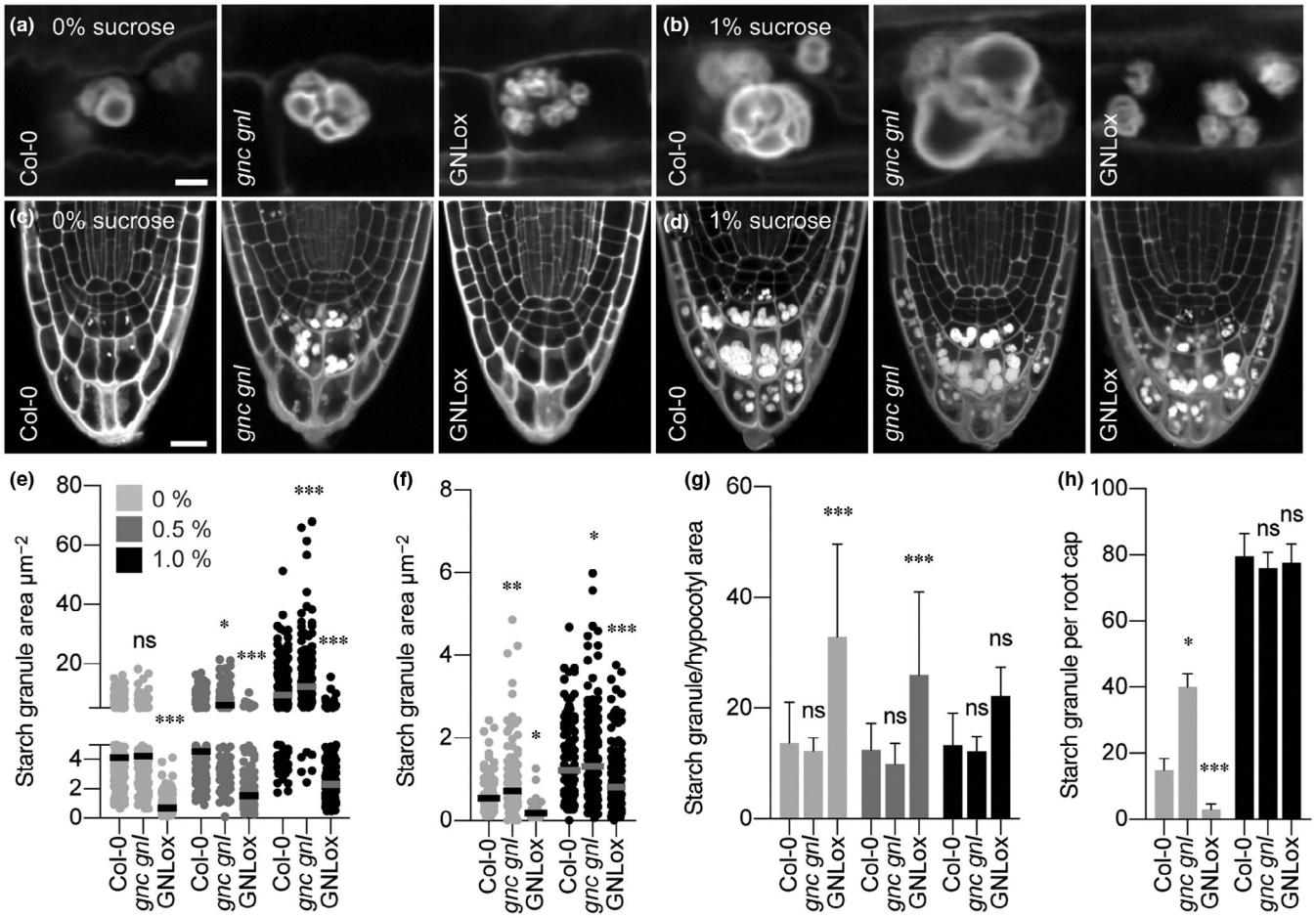

Fig. 3 GNC and GNL are repressors of starch granule growth in hypocotyl endodermal and root columella cells. (a–d) Representative confocal microscopy images of mPS-PI-stained starch granules from hypocotyl endodermis cells (a, b) and of the root tip including starch granule-containing columella cells (c, d) from 5-d-old *Arabidopsis thaliana* seedlings grown on 0% (a, c) and 1% sucrose (b, d), as specified. Bars, 5 µm (a, b) and 20 µm (c, d). (e, f) Graphs displaying the starch granule area (μm^2), as a proxy for starch granule size of individual starch granules from hypocotyl endodermis cells (a, b) and root columella cells (c, d) from 5-d-old seedlings grown on 0%, 0.5% and 1% sucrose, as specified. $n \geq 200$. Black and grey band display the average of the respective measurement. (g, h) Graphs displaying average and standard deviation of starch granule number per field from hypocotyl endodermis cells (g) and the entire root columella (h) from 5-d-old seedlings grown on 0%, 0.5% and 1% sucrose, as specified. $n \geq 10$. Student's *t*-test: *, $P \leq 0.05$; **, $P \leq 0.01$; ***, $P \leq 0.001$; ns, not significant.

type, although the number of starch granules was reduced compared to the wild-type (Fig. S2a,b,e,f,g,h). It is noteworthy that *ss4* GNLox accumulated more starch granules than *ss4* in the absence and presence of sucrose (Fig. S2h).

To investigate whether the alterations in starch granule size and number affect root bending, we conducted an analysis of negative root gravitropism in 2-d-old seedlings grown in the dark (Fig. S2i). Our results showed that *sex1*, *sex1 gnc gnl* and *sex1* GNLox had increased root bending in sucrose-free and sucrose-supplemented medium compared with the wild-type, in line with the correlation between starch accumulation in root columella cells and gravitropic root bending (Fig. S2i). In the *ss4* background, no significant differences in root gravitropism compared with the wild-type were observed (Fig. S2i). However, the addition of sucrose resulted in a substantial increase in root bending in *ss4*, *ss4 gnc gnl* and *ss4* GNLox, potentially attributed to the abnormal size of starch granules found in the columella cells of these genotypes (Fig. S2e–g,i).

GNC and *GNL* repress starch degradation at the whole seedling level

Having portrayed the role of the GATA factors in starch granule growth, both in the hypocotyl endodermal and root columella cells, it still remained to be examined whether *GNC* and *GNL* also regulate starch metabolism at the whole-seedling level. After iodine staining of entire seedlings, we did not note any obvious differences in starch accumulation between the wild-type, *gnc gnl* and GNLox (Fig. 4a). To examine the effects of the GATAs on transitory starch accumulation, we measured starch in dark-grown seedlings shifted for 2 h from sucrose-free to 1% sucrose-containing medium and then following the retransfer of these seedlings to sucrose-free medium (Fig. 4b). In this experiment, *gnc gnl* accumulated starch less efficiently (1.08 mg g^{-1} FW) than the wild-type (1.49 mg g^{-1} FW) and GNLox (1.43 mg g^{-1} FW), indicating that *GNC* and *GNL* contribute to transitory starch synthesis when examined at the whole plant level (Fig. 4b). When

the seedlings were then retransferred to sucrose-free medium, starch degradation was attenuated in GNLox over a 6 h time window when compared to the wild-type, while starch degradation in *gnc gnl* was comparable to the wild-type (Fig. 4b). However, *gnc gnl*, which had accumulated less starch on sucrose-containing medium, reached the starting levels already after 2 h on sucrose-free medium while the wild-type had not yet reached this baseline at the end of the experiment after 8 h (Fig. 4b).

In a complementary experiment, we grew seedlings on 1% sucrose-containing medium and transferred them to sucrose-free ½MS medium. The seedlings of all genotypes accumulated more starch on sucrose-containing medium (*c.* 3.8 mg g^{-1} FW) than on sucrose-free medium (*c.* 0.6 mg g^{-1} FW), but starch degradation was accelerated in *gnc gnl* and attenuated in GNLox seedlings when compared to the wild-type (Fig. 4c). Based on these observations, we concluded that the B-GATAs can repress starch degradation at the whole-seedling level.

We also examined starch accumulation at the whole plant level in the *sex1* and *ss4* backgrounds in combination with the *GATA* genotypes (Fig. S4). In line with the observations made in the wild-type background, we did not detect significant changes in starch accumulation in comparison with the respective single *sex1* or *ss4* mutants, although there were alterations in starch accumulation in *sex1* on sucrose-free medium and in *ss4* on sucrose-containing medium in the presence of the *GATA* genotypes (Fig. S4). At the adult stage, the *sex1* GNLox and ss4 GNLox mutants grew more vigorously than GNLox and its typical stunted growth was suppressed (Fig. S5; Behringer *et al.*, 2014).

Starch granule morphology is altered in the *B-GATA* genotypes

The number, size and shape of starch granules is affected by the rate of initiation and the relative abundance of amylose and amylopectin (Burgy *et al.*, 2021; Merida & Fettke, 2021). We isolated starch granules from entire 3-d-old dark-grown seedlings and examined them by scanning electron microscopy (SEM; Figs S6, S7). In line with our observations made in hypocotyl endodermal and root columella cells by microscope, starch granule size was increased in preparations from *gnc gnl*, at least when seedlings were grown on 1% sucrose, suggesting that the GATAs repress granule growth or prevent granule initiation (Figs S2a,b,g, S6a,b,g). Increased starch granule size could also be detected in *sex1 gnc gnl* and *ss4 gnc gnl*, even though granule size was already considerably enlarged in both, the *sex1* and *ss4* single mutants (Fig. S6c–f,h,i). Well in line with our previous observations, GNLox repressed granule size in the wild-type and in *sex1*, but not in *ss4* GNLox where granule size reached 10 times the size detected in the wild-type (Figs S2f,g, S6a–d,g,h). Across all

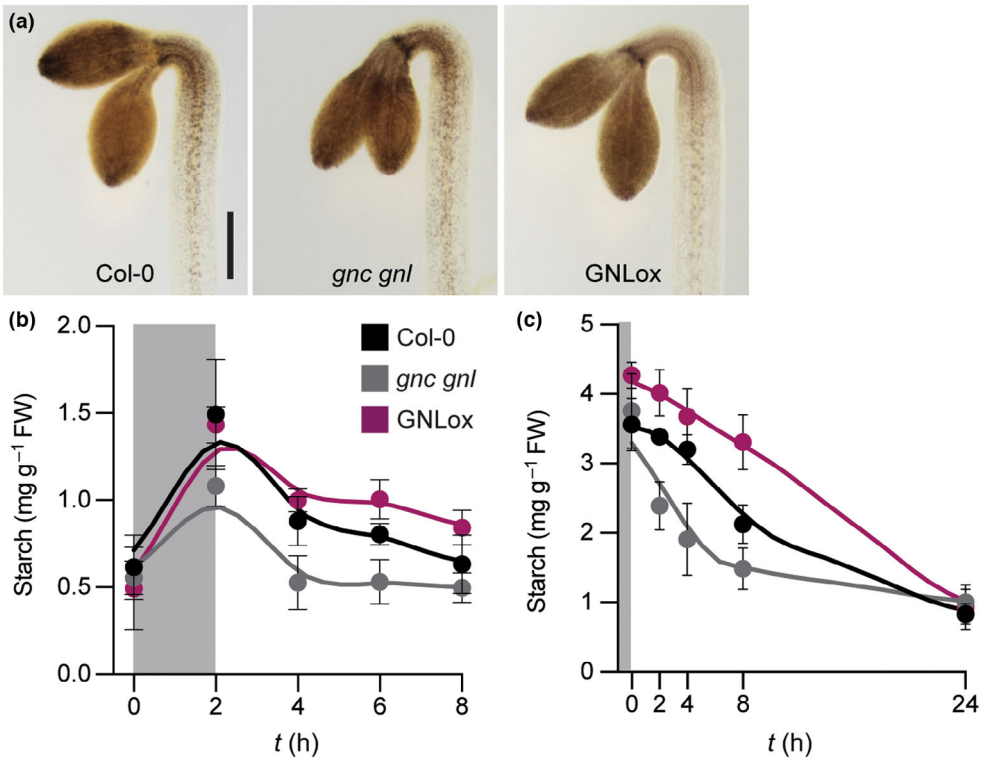

Fig. 4 *GNC* and *GNL* can act as repressors of starch degradation. (a) Representative images of 5-d-old dark-grown *Arabidopsis thaliana* seedlings grown on 1% sucrose-containing medium after starch staining with iodine. Bar, 250 μm. (b, c) Graphs displaying the average and standard deviation of starch accumulation (b) after transfer of seedlings from sucrose-free to 1% sucrose-containing medium (grey area), followed by a retransfer to sucrose-free medium (white area), or (c) from growth on 1% sucrose-containing medium (grey area) to sucrose-free medium (white area). Shown are average and standard deviation from six biological replicate samples, with each biological replicate comprising hundreds of dark-grown seedlings. Curve fitting model: point-to-point, smoothed.

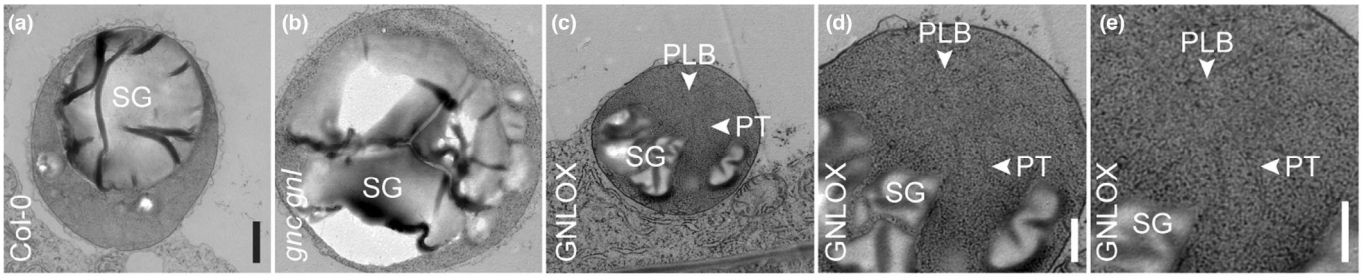

Fig. 5 GATAs can repress amyloplast differentiation. (a–e). Transmission electron microscopy images of representative amyloplasts from the hypocotyl endodermis of 5-d-old dark-grown *Arabidopsis thaliana* seedlings grown on sucrose-free medium taken at the same magnification. (d) and (e) are magnification of the image shown in (c) for better visualization of PLB and PT. PLB, prolamellar body; PT, protothylakoid; SG, starch granule. Bars: (a–c) 2 μm; (d, e) 0.5 μm.

genotypes and on both growth media tested, starch granule size was increased in the *gnc gnl* mutant, and at least in the wild-type and in *sex1* decreased in GNLox. Remarkably, in all genotypes, starch granules acquired a spherical morphology rather than the well-characterized flattened discoid morphology of granules located in cotyledons, stomata or rosette leaves of *Arabidopsis thaliana* plants (Burgy *et al.*, 2021; Liu *et al.*, 2021b; Lim *et al.*, 2022) suggesting that in the dark, starch granules adopt a spherical shape.

In addition, we noted increased fusion of multiple individual starch granules in *gnc gnl*, as well as in *sex1 gnc gnl* (Fig. S7). Interestingly, the effect on granule fusion was not observed in the *ss4 gnc gnl* mutant, indicating that granule initiation and subsequent fusion requires *SS4* activity (Fig. S7). We concluded that *GNC* and *GNL* repress starch granule growth and starch granule initiation in an *SS4*-dependent manner.

GNC and *GNL* regulate amyloplast differentiation

Like chloroplasts, amyloplasts are derived from proplastids (Jarvis & Lopez-Juez, 2013). Amyloplasts form in starch storage tissues but also in gravity-sensing root columella and hypocotyl endodermis cells. The mechanisms regulating the cell type-specific differential accumulation of amyloplasts are not understood. In view of an apparent role of the GATAs in chloroplast division and differentiation, we next examined whether the differentiation of starch-accumulating amyloplasts was affected in *gnc gnl* or in GNLox using transmission electron microscopy. Indeed, we noted that amyloplasts from the GNLox background were generally smaller and included smaller starch granules (Fig. 5). Furthermore, we noted the presence of prolamellar bodies (PLB) and protothylakoids (PT), characteristic features of etioplasts, in the GNLox amyloplasts (Fig. 5). The GATAs may thus repress amyloplast differentiation.

The effects of *GNC* and *GNL* on hypocotyl-negative gravitropism affect phototropic responses

Light induces positive phototropic hypocotyl bending, for example when dark-grown seedlings are exposed to unilateral blue light. In the light, light and gravity regulate tropic responses but the two inputs may not always act in the same direction. The transcription of *GNC* and, particularly, that of *GNL* are light-induced and the repressive effects of *GNC* and *GNL* on starch formation may weaken the relative contribution of negative hypocotyl gravitropism on tropic responses in the light (Naito *et al.*, 2007; Ranftl *et al.*, 2016). We therefore tested the contribution of the B-GATA factors to tropic responses by exposing dark-grown seedlings to a phototropic and gravitropic stimulus. In the first experiment, we illuminated the seedlings from above with blue light such that phototropic and negative gravitropic hypocotyl bending would act in the same direction. Under these conditions, all genotypes responded uniformly by strongly bending the hypocotyls towards the light and away from the gravity vector (Fig. 6a,b). In a second experiment, we provided the light from the bottom such that phototropic and gravitropic growth would antagonize each other. As expected, phototropic hypocotyl bending was dominant over negative gravitropism in this experiment (Fig. 6c,d; Hangarter, 1997). However, the *gnc gnl* mutant bent less efficiently than the wild-type, whereas GNLox bent more efficiently (Fig. 6c,d). In correlation with our observation of increased and decreased starch formation in *gnc gnl* mutants and GNLox, respectively, we reasoned that the differential starch accumulation of these mutants may be causal for their differential tropic responses. Light regulation of *GNC* and *GNL* gene expression, and their effects on starch synthesis may thus help to decrease the contribution of negative gravitropic growth at the expense of positive phototropic growth for improved photosynthesis.

Discussion

In this study, we have uncovered a novel role of the GATA factors *GNC* and *GNL* in the regulation of starch granule initiation in gravisensing cells of seedlings grown in the dark. This is reflected by the increased growth and accumulation of starch granules in hypocotyl and columella cells of *gnc gnl* double mutants, and accompanied by changes in gene expression patters (Figs 2, 3). In the dark, changes in starch granule accumulation were found to correlate with altered gravitropic responses in the hypocotyl and the root, and may also explain similar changes during gravitropism in shoots (Fig. 1). Although we cannot rule out the possibility that auxin and gibberellin may also modulate the effects of *GNC* and *GNL* on later stages of plant gravitropism,

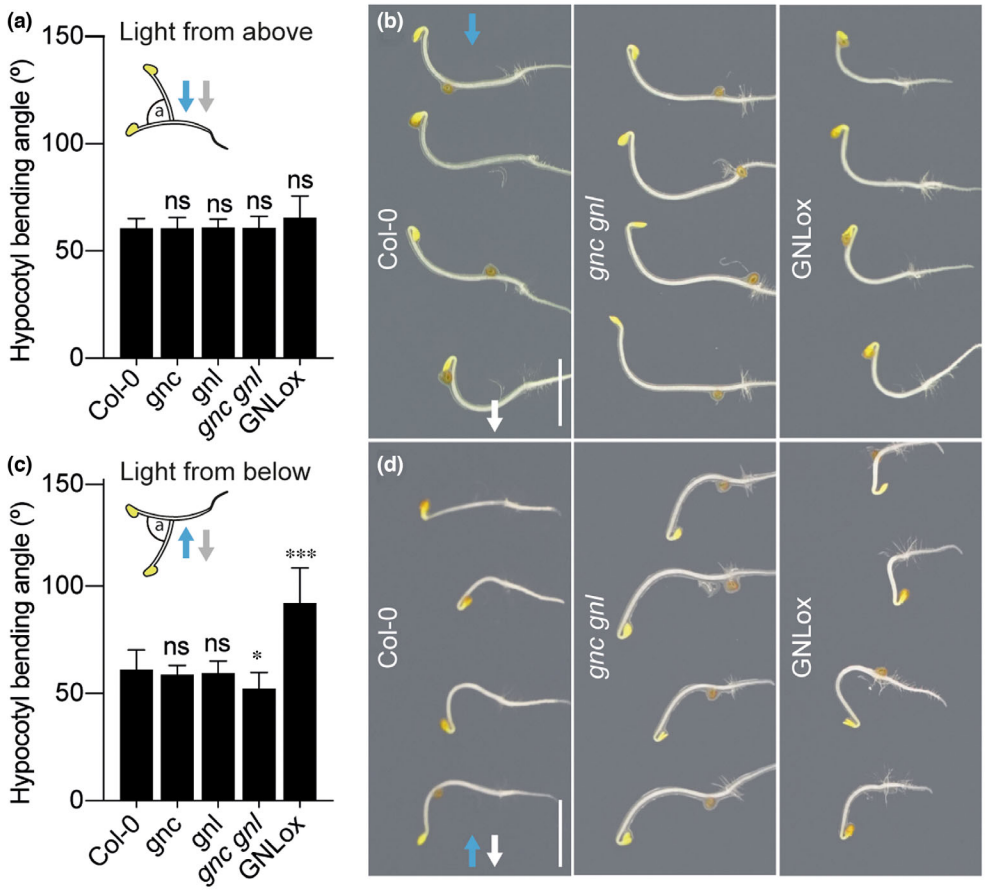

Fig. 6 Strength of phototropic responses is modulated by *GNC* and *GNL*. (a, c) Graphs displaying the average and standard deviation of hypocotyl bending angles (a) of 2-d-old dark-grown *Arabidopsis thaliana* seedlings 6 h after reorienting the seedlings by 90°. In (a), seedlings were illuminated with blue light from the top such that phototropic and negatively gravitropic hypocotyl bending would occur in the same direction. In (c), seedlings were illuminated from the bottom such that phototropic bending and negatively gravitropic bending antagonize each other. Student's *t*-test: *, $P \leq 0.01$; ***, $P \leq 0.001$; ns, not significant. (b, d) Photographs of representative seedlings from the experiments quantified in (a) and (b), respectively. Bars, 2 mm.

it is important to emphasize that the observations made in dark-grown seedlings grown without sucrose provide compelling evidence for a direct regulation of *GNC* and *GNL* on starch granule growth and thus, altered gravity perception. Furthermore, the growth and bending of seedlings were consistent across all GATA genotypes analysed (Fig. 6a,b). Taken together, these findings strongly suggest that the observed differences in gravity perception were a result of defects in starch granule growth, rather than defects in auxin polar transport.

This new role of *GNC* and *GNL* in regulating starch metabolism adds to their previously described roles of the GATA factors in regulating of chlorophyll accumulation and stomata formation. Therefore, *GNC* and *GNL* not only regulate carbon uptake by controlling photosynthesis and stomata formation, but they also regulate the storage and metabolism of the sugars formed through these processes (Chiang *et al.*, 2012; Klermund *et al.*, 2016; Bastakis *et al.*, 2018). The fact that *GNC* and *GNL* can also repress amyloplast development, as observed in the GNLox GATA overexpression line, in conjunction with the previously described role in chloroplast development, positions *GNC* and *GNL*, more generally, as regulators of plastid differentiation (Fig. 5; Chiang *et al.*, 2012).

The intricate regulation of starch metabolism and starch granule initiation remains a subject of ongoing research, with much still to be elucidated (Merida & Fettke, 2021; Apriyanto *et al.*, 2022). Recent studies have shown that starch synthesis, degradation and starch granule initiation are interconnected processes, making it difficult to investigate each process independently (Seung *et al.*, 2018; Liu *et al.*, 2021a; Muntaha *et al.*, 2022). Our results highlight that these processes occur simultaneously, as evidenced by our experiments. Our research focusses on the growth of starch granules in endodermal and columella cells of seedlings grown in the dark (Figs 1–3). This approach allows us to use tropic responses as a physiological readout of the observed changes in starch accumulation and avoid the confounding effects of photosynthesis during day-night cycles, transitory starch synthesis and degradation, or differential sugar distribution through sugar transport (Zeeman *et al.*, 2002).

When analysed at the whole seedling level, we observed that the GATA factors have a more complex role in regulating starch synthesis, degradation, granule initiation and morphology, which became even more complex in the *sex1* and *ss4* backgrounds (Figs 4, S2, S6, S7). The individual processes may involve several feedback regulatory mechanisms, which could be disturbed in the

GATA genotypes when examined in the wild-type or in their genetic interplay with *SEX1* and *SS4*.

Through the combination of different microscopy techniques, we were able to observe compound granules in *gnc gnl*, which were further intensified in *sex1 gnc gnl* (Fig. S7), but not in *ss4 gnc gnl*. This finding is consistent with a recent study that suggests that in the *ss4* single mutant, starch is deposited almost uniformly due to no simultaneous initiations (Burgy *et al.*, 2021). In the wild-type, starch is believed to expand in an anisotropic manner, fusing together into a final starch granule (Burgy *et al.*, 2021). However, the compound granules observed in *gnc gnl* and *sex1 gnc gnl* seedlings do not completely fuse together (Fig. S7). Instead, the shape of individual granules within a compound granule resemble initiation models described in the endosperm of cereals (Hawkins *et al.*, 2021).

Changes in starch accumulation had previously been observed in GATA backgrounds but the underlying mechanisms were neither studied nor rationalised (Hudson *et al.*, 2013). We argue that the differential effects of the GATAs in these genotypes may be the effect of disturbances of these phenotypes and of effects taking place at the individual cell and tissue level that cannot be resolved when examining entire seedlings.

After the transition from skotomorphogenic to photomorphogenic growth, plants mainly respond to the phototropic stimulus and the contribution of negative gravitropism for shoot growth becomes secondary. The transcriptional upregulation of *GNC* and *GNL* in the light may contribute to photomorphogenic growth not only by promoting greening and photosynthesis but also by repressing starch synthesis and gravitropism responses. Our work uncovers an important role of GNC and GNL in the regulation of an important process in primary metabolism in plants and highlights the role of the GATAs in mediating between these metabolic processes and related growth adaptations.

Acknowledgements

The authors would to acknowledge technical support by Dominik Fiedler from the Fraunhofer Institute for Process Engineering and Packaging for assistance with scanning electron microscopy, as well as funding by the Deutsche Forschungsgemeinschaft through grants-in-aid DFG SCH751/9-2 and DFG SCHW751/19-1 to CS. Open Access funding enabled and organized by Projekt DEAL.

Competing interests

None declared.

Author contributions

JS, NM, EI and CS designed the experiments. JS performed all experiments, except for the TEM analysis. NM performed the TEM analysis. JS and CS wrote the manuscript. NM and EI edited and approved the manuscript.

ORCID

Erika Isono https://orcid.org/0000-0002-3754-8964
Niccolò Mosesso https://orcid.org/0000-0002-3590-8698
Jan Sala https://orcid.org/0000-0002-8896-1265
Claus Schwechheimer https://orcid.org/0000-0003-0269-2330

Data availability

The RNAseq data that support the findings of this study are available at Gene Expression Omnibus (https://www.ncbi.nlm.nih.gov/geo/) under accession no. GSE205524.

References

Apriyanto A, Compart J, Fettke J. 2022. A review of starch, a unique biopolymer – structure, metabolism and in planta modifications. *Plant Science* **318**: 111223.

Ashburner M, Ball CA, Blake JA, Botstein D, Butler H, Cherry JM, Davis AP, Dolinski K, Dwight SS, Eppig JT *et al.* 2000. Gene ontology: tool for the unification of biology. The Gene Ontology Consortium. *Nature Genetics* **25**: 25–29.

Bastakis E, Hedtke B, Klermund C, Grimm B, Schwechheimer C. 2018. LLM-domain B-GATA transcription factors play multifaceted roles in controlling greening in Arabidopsis. *Plant Cell* **30**: 582–599.

Behringer C, Bastakis E, Ranftl QL, Mayer KF, Schwechheimer C. 2014. Functional diversification within the family of B-GATA transcription factors through the leucine-leucine-methionine domain. *Plant Physiology* **166**: 293–305.

Bi YM, Zhang Y, Signorelli T, Zhao R, Zhu T, Rothstein S. 2005. Genetic analysis of Arabidopsis GATA transcription factor gene family reveals a nitrate-inducible member important for chlorophyll synthesis and glucose sensitivity. *The Plant Journal* **44**: 680–692.

Briggs WR, Christie JM. 2002. Phototropins 1 and 2: versatile plant blue-light receptors. *Trends in Plant Science* **7**: 204–210.

Burgy L, Eicke S, Kopp C, Jenny C, Lu KJ, Escrig S, Meibom A, Zeeman SC. 2021. Coalescence and directed anisotropic growth of starch granule initials in subdomains of *Arabidopsis thaliana* chloroplasts. *Nature Communications* **12**: 6944.

Chiang YH, Zubo YO, Tapken W, Kim HJ, Lavanway AM, Howard L, Pilon M, Kieber JJ, Schaller GE. 2012. Functional characterization of the GATA transcription factors GNC and CGA1 reveals their key role in chloroplast development, growth, and division in Arabidopsis. *Plant Physiology* **160**: 332–348.

Christie JM, Murphy AS. 2013. Shoot phototropism in higher plants: new light through old concepts. *American Journal of Botany* **100**: 35–46.

Crumpton-Taylor M, Pike M, Lu KJ, Hylton CM, Feil R, Eicke S, Lunn JE, Zeeman SC, Smith AM. 2013. Starch synthase 4 is essential for coordination of starch granule formation with chloroplast division during Arabidopsis leaf expansion. *New Phytologist* **200**: 1064–1075.

Delvalle D, Dumez S, Wattebled F, Roldan I, Planchot V, Berbezy P, Colonna P, Vyas D, Chatterjee M, Ball S *et al.* 2005. Soluble starch synthase I: a major determinant for the synthesis of amylopectin in *Arabidopsis thaliana* leaves. *The Plant Journal* **43**: 398–412.

Edner C, Li J, Albrecht T, Mahlow S, Hejazi M, Hussain H, Kaplan F, Guy C, Smith SM, Steup M *et al.* 2007. Glucan, water dikinase activity stimulates breakdown of starch granules by plastidial β-amylases. *Plant Physiology* **145**: 17–28.

Feike D, Pike M, Gurrieri L, Graf A, Smith AM. 2022. A dominant mutation in *β-AMYLASE1* disrupts nighttime control of starch degradation in Arabidopsis leaves. *Plant Physiology* **188**: 1979–1992.

Flutsch S, Wang Y, Takemiya A, Vialet-Chabrand SRM, Klejchova M, Nigro A, Hills A, Lawson T, Blatt MR, Santelia D. 2020. Guard cell starch degradation

yields glucose for rapid stomatal opening in Arabidopsis. *Plant Cell* **32**: 2325–2344.

Gamez-Arjona FM, Merida A. 2021. Interplay between the N-terminal domains of *Arabidopsis* starch synthase 3 determines the interaction of the enzyme with the starch granule. *Frontiers in Plant Science* **12**: 704161.

Gene Ontology, C. 2021. The gene ontology resource: enriching a GOld mine. *Nucleic Acids Research* **49**: D325–D334.

Hangarter RP. 1997. Gravity, light and plant form. *Plant, Cell & Environment* **20**: 796–800.

Hawkins E, Chen J, Watson-Lazowski A, Ahn-Jarvis J, Barclay JE, Fahy B, Hartley M, Warren FJ, Seung D. 2021. STARCH SYNTHASE 4 is required for normal starch granule initiation in amyloplasts of wheat endosperm. *New Phytologist* **230**: 2371–2386.

Hudson D, Guevara DR, Hand AJ, Xu Z, Hao L, Chen X, Zhu T, Bi YM, Rothstein SJ. 2013. Rice cytokinin GATA transcription factor1 regulates chloroplast development and plant architecture. *Plant Physiology* **162**: 132–144.

Jarvis P, Lopez-Juez E. 2013. Biogenesis and homeostasis of chloroplasts and other plastids. *Nature Reviews. Molecular Cell Biology* **14**: 787–802.

Khurana JP, Best TR, Poff KL. 1989. Influence of hook position on phototropic and gravitropic curvature by etiolated hypocotyls of *Arabidopsis thaliana*. *Plant Physiology* **90**: 376–379.

Kiss JZ. 2000. Mechanisms of the early phases of plant gravitropism. *Critical Reviews in Plant Sciences* **19**: 551–573.

Kiss JZ, Guisinger MM, Miller AJ. 1998. What is the threshold amount of starch necessary for full gravitropic sensitivity? *Advances in Space Research* **21**: 1197–1202.

Kiss JZ, Hertel R, Sack FD. 1989. Amyloplasts are necessary for full gravitropic sensitivity in roots of *Arabidopsis thaliana*. *Planta* **177**: 198–206.

Klermund C, Ranftl QL, Diener J, Bastakis E, Richter R, Schwechheimer C. 2016. LLM-domain B-GATA transcription factors promote stomatal development downstream of light signaling pathways in *Arabidopsis thaliana* hypocotyls. *Plant Cell* **28**: 646–660.

Lamesch P, Berardini TZ, Li D, Swarbreck D, Wilks C, Sasidharan R, Muller R, Dreher K, Alexander DL, Garcia-Hernandez M *et al.* 2012. The Arabidopsis Information Resource (TAIR): improved gene annotation and new tools. *Nucleic Acids Research* **40**: D1202–D1210.

Lim SL, Flutsch S, Liu J, Distefano L, Santelia D, Lim BL. 2022. Arabidopsis guard cell chloroplasts import cytosolic ATP for starch turnover and stomatal opening. *Nature Communications* **13**: 652.

Liu Q, Li X, Fettke J. 2021a. Starch granules in *Arabidopsis thaliana* mesophyll and guard cells show similar morphology but differences in size and number. *International Journal of Molecular Sciences* **22**: 5666.

Liu Q, Zhou Y, Fettke J. 2021b. Starch granule size and morphology of *Arabidopsis thaliana* starch-related mutants analyzed during diurnal rhythm and development. *Molecules* **26**: 5859.

Lu KJ, Streb S, Meier F, Pfister B, Zeeman SC. 2015. Molecular genetic analysis of glucan branching enzymes from plants and bacteria in Arabidopsis reveals marked differences in their functions and capacity to mediate starch granule formation. *Plant Physiology* **169**: 1638–1655.

Mahlow S, Hejazi M, Kuhnert F, Garz A, Brust H, Baumann O, Fettke J. 2014. Phosphorylation of transitory starch by α-glucan, water dikinase during starch turnover affects the surface properties and morphology of starch granules. *New Phytologist* **203**: 495–507.

Merida A, Fettke J. 2021. Starch granule initiation in *Arabidopsis thaliana* chloroplasts. *The Plant Journal* **107**: 688–697.

Muntaha SN, Li X, Compart J, Apriyanto A, Fettke J. 2022. Carbon pathways during transitory starch degradation in Arabidopsis differentially affect the starch granule number and morphology in the *dpe2/phs1* mutant background. *Plant Physiology and Biochemistry* **180**: 35–41.

Naito T, Kiba T, Koizumi N, Yamashino T, Mizuno T. 2007. Characterization of a unique GATA family gene that responds to both light and cytokinin in *Arabidopsis thaliana*. *Bioscience, Biotechnology, and Biochemistry* **71**: 1557–1560.

Ranftl QL, Bastakis E, Klermund C, Schwechheimer C. 2016. LLM-domain containing B-GATA factors control different aspects of cytokinin-regulated development in *Arabidopsis thaliana*. *Plant Physiology* **170**: 2295–2311.

Richter R, Behringer C, Muller IK, Schwechheimer C. 2010. The GATA-type transcription factors GNC and GNL/CGA1 repress gibberellin signaling downstream from DELLA proteins and PHYTOCHROME-INTERACTING FACTORS. *Genes & Development* **24**: 2093–2104.

Roldan I, Wattebled F, Mercedes Lucas M, Delvalle D, Planchot V, Jimenez S, Perez R, Ball S, D'Hulst C, Merida A. 2007. The phenotype of soluble starch synthase IV defective mutants of *Arabidopsis thaliana* suggests a novel function of elongation enzymes in the control of starch granule formation. *The Plant Journal* **49**: 492–504.

Sato EM, Hijazi H, Bennett MJ, Vissenberg K, Swarup R. 2015. New insights into root gravitropic signalling. *Journal of Experimental Botany* **66**: 2155–2165.

Schindelin J, Arganda-Carreras I, Frise E, Kaynig V, Longair M, Pietzsch T, Preibisch S, Rueden C, Saalfeld S, Schmid B *et al.* 2012. Fiji: an open-source platform for biological-image analysis. *Nature Methods* **9**: 676–682.

Schwechheimer C, Schroder PM, Blaby-Haas CE. 2022. Plant GATA factors: their biology, phylogeny, and phylogenomics. *Annual Review of Plant Biology* **73**: 123–148.

Seung D. 2020. Amylose in starch: towards an understanding of biosynthesis, structure and function. *New Phytologist* **228**: 1490–1504.

Seung D, Echevarria-Poza A, Steuernagel B, Smith AM. 2020. Natural polymorphisms in Arabidopsis result in wide variation or loss of the amylose component of starch. *Plant Physiology* **182**: 870–881.

Seung D, Schreier TB, Burgy L, Eicke S, Zeeman SC. 2018. Two plastidial coiled-coil proteins are essential for normal starch granule initiation in Arabidopsis. *Plant Cell* **30**: 1523–1542.

Shannon P, Markiel A, Ozier O, Baliga NS, Wang JT, Ramage D, Amin N, Schwikowski B, Ideker T. 2003. Cytoscape: a software environment for integrated models of biomolecular interaction networks. *Genome Research* **13**: 2498–2504.

Szklarczyk D, Morris JH, Cook H, Kuhn M, Wyder S, Simonovic M, Santos A, Doncheva NT, Roth A, Bork P *et al.* 2017. The STRING database in 2017: quality-controlled protein-protein association networks, made broadly accessible. *Nucleic Acids Research* **45**: D362–D368.

Truernit E, Bauby H, Dubreucq B, Grandjean O, Runions J, Barthelemy J, Palauqui JC. 2008. High-resolution whole-mount imaging of three-dimensional tissue organization and gene expression enables the study of Phloem development and structure in Arabidopsis. *Plant Cell* **20**: 1494–1503.

Yu TS, Kofler H, Hausler RE, Hille D, Flugge UI, Zeeman SC, Smith AM, Kossmann J, Lloyd J, Ritte G *et al.* 2001. The Arabidopsis *sex1* mutant is defective in the R1 protein, a general regulator of starch degradation in plants, and not in the chloroplast hexose transporter. *Plant Cell* **13**: 1907–1918.

Zeeman SC, Tiessen A, Pilling E, Kato KL, Donald AM, Smith AM. 2002. Starch synthesis in Arabidopsis. Granule synthesis, composition, and structure. *Plant Physiology* **129**: 516–529.

Zhang X, Szydlowski N, Delvalle D, D'Hulst C, James MG, Myers AM. 2008. Overlapping functions of the starch synthases SSII and SSIII in amylopectin biosynthesis in Arabidopsis. *BMC Plant Biology* **8**: 96.

Zubo YO, Blakley IC, Franco-Zorrilla JM, Yamburenko MV, Solano R, Kieber JJ, Loraine AE, Schaller GE. 2018. Coordination of chloroplast development through the action of the GNC and GLK transcription factor families. *Plant Physiology* **178**: 130–147.

Supporting Information

Additional Supporting Information may be found online in the Supporting Information section at the end of the article.

Fig. S1 *GNC* and *GNL* repress starch granule growth in hypocotyl endodermal cells.

Fig. S2 *GNC* and *GNL* genetically interact with *GWD1*/*SEX1* (*glycan water dikinase1*/*STARCH EXCESS1*) and *SS4* (*STARCH SYNTHASE4*).

Fig. S3 Starch granule accumulation in *sex1* and *sex1* GNLox roots.

Fig. S4 Differential effects of *GNC* and *GNL* on starch accumulation at the whole plant level in the *sex1* and *ss4* backgrounds.

Fig. S5 Adult plant phenotypes of genetic interaction study with *SEX1* and *SS4*.

Fig. S6 *GNC* and *GNL* repress starch granule growth.

Fig. S7 *GNC* and *GNL* repress granule budding.

Table S1 List of primers used for PCR-based genotyping.

Table S2 Differentially expressed genes in the *gnc gnl* mutant and the GNLox overexpressor.

Table S3 Differentially expressed genes from *gnc gnl* belonging to the five most prominent GO terms categories.

Please note: Wiley is not responsible for the content or functionality of any Supporting Information supplied by the authors. Any queries (other than missing material) should be directed to the *New Phytologist* Central Office.